Biophysical Journal

The role of peptide conformation presented by MHC in the induction of TCR triggering

--Manuscript Draft--

Manuscript Number:	BIOPHYSICAL-JOURNAL-D-24-00450R1
Full Title:	The role of peptide conformation presented by MHC in the induction of TCR triggering
Short Title:	Role of peptide in TCR triggering
Article Type:	Regular Article
Corresponding Author:	Yuri Sykulev Thomas Jefferson University Philadelphia, PA UNITED STATES
Order of Authors:	Yuri Sykulev
	Andrey V Golovin
	Sergey Panteleev
	Alexander S Zlobin
	Nadia Anikeeva
	Ivan Smirnov
	Alexander Gabibov
Abstract:	High resolution crystal structure of stimulatory peptide-MHC (pMHC) ligands bound to TCR revealed different conformation of the two peptides at positions P6 and V7 compared to the conformation of the same peptides presented by unliganded MHC. Supercomputer simulation and well-tempered metadynamics approach revealed several meta-stable non-canonical TCR-pMHC interactions that depend on the conformation of the MHC-bound peptides. The diversity of meta-stable states was significantly more represented in signaling TCR-pMHC complex. These findings suggest that TCR-pMHC recognition can be informed by a conformation of peptide presented by MHC that notably influences the orientation of TCR recognizing pMHC ligand. It appears that TCR bound to stimulatory pMHC possess a significantly higher degree of freedom to assume various metastable TCR orientations which are distinct from canonical docking. In contrast, TCR interacting with non-stimulatory pMHC ligand revealed markedly less meta-stable non-canonical interactions and disengaged from the pMHC. This suggests that productive TCR-mediated signaling may depend on non-canonical interactions between TCR and pMHC, either facilitating early recognition events or providing new contacts for catch-bond formation. Our discovery can inform future attempts to simulate the catch-bond formation mechanism in TCR-pMHC recognition, allowing the formation of new bonds mediating alternative peptide presentation.
Secondary Abstract:	How TCR discriminates between stimulatory and non-stimulatory peptide-MHC (pMHC) ligands is not understood. We have applied well-tempered metadynamics and supercomputing to reveal several meta-stable non-canonical TCR-pMHC interactions that depend on the conformation of MHC-bound peptides. Modeling of possible TCR orientations relative to stimulatory pMHCs uncovered metastable TCR positioning that are likely characterized by different stability of the TCR-pMHC complex. The analysis revealed a unique metastable TCRs orientation bound to stimulatory pMHCs that was not evident for TCRs interacting with non-stimulatory pMHC ligands. This suggests that establishing a unique metastable TCR position relative to MHC is required for TCR triggering and has not been previously observed.
Suggested Reviewers:	Brian Baker brian-baker@nd.edu
	Balbino Alarcon balarcon@cbm.csic.es
	Giovanni Bussi bussi@sissa.it

Opposed Reviewers:	

Dear Editor

My colleagues and I are pleased to submit our manuscript entitled “The role of peptide conformation presented by MHC in the induction of TCR triggering” for publication in Biophysical Journal.

While crystal structure identifies all visible bonds stabilizing TCR-pMHC complex, it cannot explain a possible mechanism of TCR triggering. Indeed, the structures of stimulatory and non-stimulatory TCR-pMHC complexes has been found to be essentially identical. To unravel the mechanism of TCR triggering, we have utilized supercomputing modeling and metadynamics approach to reconstruct all possible TCR orientations relative to pMHC surface from available crystal structures of syngeneic and allogeneic TCR bound to either stimulatory or non-stimulatory pMHC ligands. We compared canonical docking states with intermediate docking states for the TCR-pMHC complexes and revealed a unique metastable orientation in the stimulatory complexes. This unique metastable orientation indicates a clear difference between stimulatory and non-stimulatory TCR-pMHC complexes. We believe that these findings allows us to propose a model that explains how TCR discriminates between various pMHC ligands and triggers TCR-mediate signaling.

We would like to suggest the following reviewers:

Brian Baker, University of Notre Dame, email - brian-baker@nd.edu
David Margulies, National Institute of Health, email - david.margulies@nih.gov
Eric Martinez-Hackert, Michigan State University, email - emh@msu.edu
Balbino Alarcon, Universidad Autónoma de Madrid, email – balarcon@cbm.csic.es
Diana Gil Pages, University of Missouri, email- GilPagesd@health.missouri.edu
Zoe Cournia, Biomedical Research Foundation, Academy of Athens, email - zcournia@bioacademy.gr
Vittorio Limongelli, Università della Svizzera italiana: Lugano, CH, email - vittorio.limongelli@usi.ch

Giovanni, Bussi, Scuola Internazionale Superiore di Studi Avanzati, Trieste, Italy, email – bussi@sissa.it

Respectfully,

Yuri Sykulev

To the Editor
Biophysical Journal

Dear Editor

We are grateful to reviewers for the in-depth analysis of our manuscript and useful comments. They believe that the proposed analysis revealed a unique metastable TCR orientation bound to stimulatory pMHC ligand, which was not observed for TCR interacting with non-stimulatory pMHC ligand. In addition, the reviewers raised number of issues requiring changes in presentation of experimental data that is necessary to support the conclusions.

We systematically addressed all reviewers' questions and provided detailed answers and clarifications. All changes in the revised manuscript have been highlighted in red. We believe that all these changes provided necessary clarifications. As a result, the revised manuscript has been significantly improved, and we hope that the manuscript will now be considered for publication in Biophysical Journal.

Below are point-by-point answers to reviewers' questions.

Reviewer #1

1. The authors through that the text identifies a set of simulation trajectory as "supercomputer simulation". This raises a question, namely, are the authors referring to equilibrium molecular dynamics simulations? If yes, how long these simulations were performed and how many replicates have been determined?

Answer: We performed biased molecular dynamics, namely metadynamics simulations with funnel potential. Meta-dynamic was run in two steps. First, an exploration run was performed for 1 μs. Followed by the production runs for every system, the final metadynamics trajectory amounted to 15 μs with six mpi walkers each of 2.5 μs. Convergences of simulation are presented in Supplementary Figures 5 and 6.

2. The order of text in this manuscript for critical details such as initial structural model, molecular dynamics methodology details fall short to the standards of Biophysical Journal. For instance, in the section "Model," the authors included details about the structure of the TCR-pMHC interface at high resolution with reference to the accession code/codes. It was confusing weather this was an experimentally determined structure or generated by a deep-learning algorithm. Note, both can be at high resolution. The reviewer suggests rearranging the text stating clearly what are characteristics of the starting model that has been used for simulation. This is important to ensure that there is no initial model bias towards the claims and conclusions in the manuscript

Answer: In the section “Model,” we provided information about the structure of the TCR-pMHC interface derived from published high-resolution X-ray crystallographic data. This allows comparison of the structure derived from X-ray crystallographic data with the structure attained from computational analysis. In metadynamics simulations from our Exploration runs (based on X-ray data), we identified 6 minima corresponding to non-X-ray states. These minima were then used as starting states for Production runs (independent of X-ray data). Thus, our simulations reproduced contacts found in X-ray data as well as identify intermediate metastable states.

Questions 3 and 9 *touch on similar topics and require similar answer. Both questions are listed below back-to back, and our response aims to answer both questions.*

3. Analyzing the present work, I found that the author’s choice imposing positional restraints to the C-alpha atoms in MHC is ambiguous. The authors stated that this choice was to avoid inappropriate orientations between interacting pMHC ligands and TCR. I was concerned that the authors choice could have an impact of the final result. Speaking succinctly, how limitation of the degree of freedom (DOF) to a certain range impacts the free energy surface plots (Figure 8 and supplementary Figure 1). My interpretation (based on Fig. 1 caption) of the authors simulation design is that restraints of MHC were applied to restrict (or make the domain stiff) or to improve sampling efficiency between TCR-MHC. However, is this scenario physiologically relevant? Detailed clarification relating this choice to physiology is necessary.

9. In relation to my earlier comment on the restrained DOF, how was ~ 35 degrees considered physiologically relevant? Also, how did the authors determine 1000 kJ/(au . mol) restraint applied to MHC corresponds to ~ 35 degrees? Has this been quantified from a equilibrium trajectory? Please include the time-series plot in the manuscript.

Answer: 1000 $[\frac{kJ}{au^2 \times mol}]$, is a soft limit allowing an efficient sampling that includes values up to 35 degrees of TCR tilt. Only C-alpha atoms of the **beta-sheet** in the MHC were restricted. This accounts for physiological restriction on MHC movement: MHC is anchored to the membrane by a transmembrane domain and is tightly clustered. No restrictions were applied to MHC helixes that are responsible for TCR interaction. Our goal was to focus on peptide-specific physiologically relevant TCR-pMHC interaction at the interface, specifically during the early stages of TCR-pMHC engagement following initial recognition events. TCR-pMHC interactions proceed in the context of constrained space between target and effector cell membranes. Both TCR and pMHC are also present on the surface of the membrane as clusters thus facilitating mostly vertical orientation. This, in turn, limits physiologically relevant TCR tilt from the normal vector to the pMHC surface. According to Singh et al., Proteins. 2019;88:503–513, in physiologically

derived TCR-pMHC complexes incidence angles don't exceed ~35 degrees. We conclude that in our analysis limitations reflect physiological conditions.
The tilt angle analysis below was performed with the same settings as described for metadynamics simulation in the main methods but utilized equilibrium trajectories for plumed driver routine.

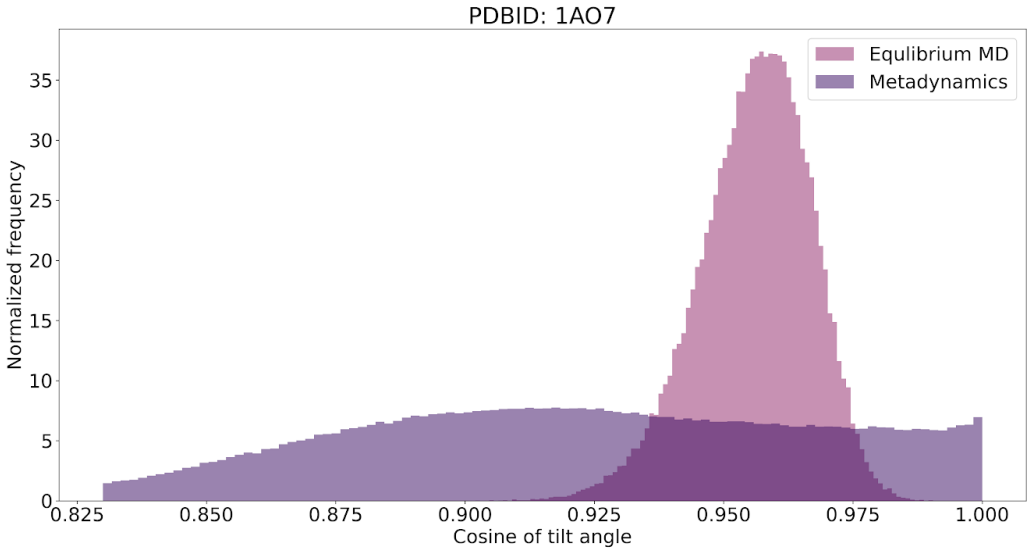

Histogram analysis of values of the tilt angle (scheme on Fig 1) in equilibrium simulation molecular dynamics and in metadynamics simulation of TCR-peptide-MHC binding process.

4. Related to my previous comment, have the authors performed simulation with different force constants - when restraining C-alpha atoms in MHC, on the impact it has on the free energy surface? Alternately, and more importantly, have the authors started with different conformations (meaning different orientations of THC) to ensure that current results do not include initial model bias? I would urge the latter to be included, to ensure the identified metastable conformations are indeed observed across multiple replicates. In fact, authors mention that they started from "6 different non-X-ray states". What are these states? Please indicate and it would be better if you can include this as a schematic diagram in one of the figures.

Answer:
For each system, we made a separate run with a trajectory length of about 6 μs, under the same conditions. We call this run an "exploration run". For these runs, we plotted the FES as a function of the distance between the centers of mass of the proteins and the torsional angle of TCR rotation relative to the MHC. We selected 6 positions of TCR bound to pMHC with minimum energy and used the conformations in these minima as starting states for "production runs"; this provided a basis to derive the main results. Supplementary Figure 3

5. The free energy surface plots are pixelated, and certain key features in terms of barriers and wells are unclear. Please include a clearer image

Answer: New hi-resolution images have been produced

6. In Fig. 3, how were states classified as metastable from metadynamics simulations? Please provide details on how the free energy surfaces were analyzed; was this based on population statistics between ensemble members, the clustering algorithm, which finally led to a conformation indicating the long-lived state in biased sampling trajectory.

Answer: In our first assumption, we considered the X-ray-derived state as the global minimum, and any other state found in metadynamics simulation as an intermediate metastable state. To be more precise, we used a reweighting-based approach: state extraction was performed from chosen conformations that belong to minima determined by selected CVs (distance and RMSD). For each state, the weight was determined by superimposed bias as in Tiwary reweighing. The states were clustered using GROMACS with a 0.3 nm cutoff and the clusters populations were reweighed. The most populated cluster was declared as a metastable state. The procedure was performed using Python and nupmy in Jupyter notebook.

7. What was the lifetime of the hydrogen bond between β-CDR1 and Y8 of the TAX peptide (Figure 2C) in the equilibrium trajectory? Can you include a time series plot?

Answer:
We used equilibrium molecular dynamics simulation as reference for biased dynamics, to estimate tilt angle (see question 3 and 9) and h-bond lifetime. The hydrogen bond between β-CDR1 and Y8 of the TAX peptide was analyzed with the MDAnalysis module for Python [Beckstein et al., 2009. *J Mol Biol*. 394:160-176] as described in the documentation. Results of this analysis on Supplementary Figures 1 and 2. We may conclude that hbond survived well in trajectory with length 1μs

8. This sentence is incomplete: "To effectively scan possible interactions between the TCR loops and the MHC surface with the presented peptide, we utilized well-tempered metadynamics in Gromacs (37) with the Plumed plugin where we used two CV's, TCR position on XY plane. "What is the other CV? Collective variable?

Answer:
The sentence was revised: To effectively scan possible interactions between the TCR loops and the MHC surface with the presented peptide, we utilized well-tempered metadynamics in Gromacs (Darden et al., *J. Phys. Chem.* 98:10089.) with the Plumed plugin where we used two collective variables X and Y

coordinates of TCR Center Of Mass interacting with the pMHC surface that defines the XY plane.

9. See above in answer to question 3

10. In sub-section production runs, the authors use 'mks'. What is mks? See, "Each walker ran for 2.5 mks with a 2-fs time step, resulting in a 15 mks trajectory for every system."

Answer:
Originally, “mks” stood for microseconds (μs). The sentence has been corrected - "Each of the six walker runs had a trajectory length of 2.5 μs with a 2-fs time step resulting in a 15 μs metadynamics trajectory length for every system."

11. Please include the convergence analysis for the free energy as part of the SI.

Answer:
New graphs for convergence shown in Supplemental Figures 5 and 6

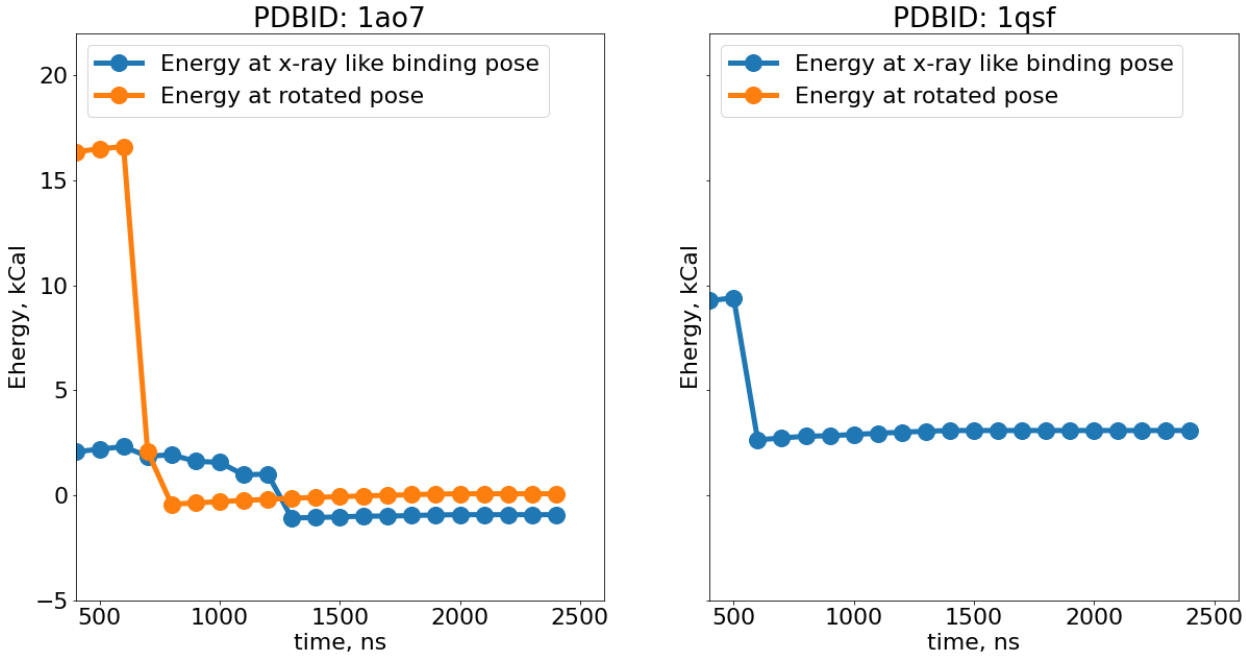

12. TIP3P water model needs citation. "Cl-"; "-" should be a superscript. Include details about electrostatic calculations, cutoff for non-bonded interactions? Also, I would rename the sub-section "system setup" to system setup for enhanced sampling or similar.

Answer:
We used Amber forcefield with explicit solvent simulations (Lindortt-Larsen at al., Proteins, 2010; 78:1950–1958) that were performed at T = 300 K under control of

velocity rescaling thermostat (Bussi et al., J. Chem. Phys. 2007, 126: 74101), with isotropic constant pressure boundary conditions under the control of the Berendsen algorithm of pressure coupling (Berendsen et al, J. Chem. Phys. 1984; 81:3684–3690), and application of particle mesh Ewald (Darden et al., J. Chem. Phys. 1993; 98:10089–10092) method for long-range electrostatics interactions (PME) with short and long-range cutoff radius 0.9nm and the same cutoff radius for VdW interaction.

13. In various analyses I did not find any analysis that is indicative of catch bonds or their lifetimes. However, that is the strongest point in the abstract. Please clarify.

Answer: The mechanism of catch bond formation is not entirely clear. It has been shown that the application of physical force from 8 to 15 pN to a cognate TCR-pMHC complex results in the development of catch bonds. The application of physical force to the non-cognate TCR-pMHC complex results in the formation of a slip bond, leading to the dissociation of the complex. Thus, the application of physical force to pMHC-bound TCR may distinguish between short-lived non-cognate and longer-lasting cognate TCR-pMHC contacts. It is likely that catch-bond formation will irreversibly denature engaged TCR. In fact, it has been shown that T cell recognition of a strong pMHC ligand on target cells results in irreversible TCR endocytose and leads to a significant decrease of the level of TCR on the surface of T cell attacking target cell (Valitutti et all, 1995, Nature).

We have found approximately 150 degrees deep TCR turn relative to stimulatory pMHC, while the same analysis of non-stimulatory TCR-pMHC interaction did not reveal similar TCR turn but led to a formation of different TCR orientation over the non-stimulatory pMHC. This may suggest that recognition of non-stimulatory pMHC may not lead to particular TCR CDR loop engagement that would facilitate TCR triggering. Consistent with this we observed significant changes in the structure of the cognate pMHC interface bound to the TCR, namely, dramatic changes of the C-terminal end bound to MHC peptide that were not evident in the interface of non-cognate pMHC. We would like to suggest that a dramatic TCR reorientation over pMHC was found only in the syngeneic signaling complex, indicating that TCR triggering likely involves the formation of non-canonical TCR-pMHC interactions. This may facilitate rapid pMHC recognition by improving the kinetics of the TCR-pMHC interaction or contribute to catch-bond formation under mechanical stress.

Reviewer #2

While the study offers valuable insights, the clarity of the results and the justification for certain methodological choices could be improved.

1. The authors should provide a more explicit justification for the selection of collective variables (CVs), addressing their interdependence and ensuring that they adequately capture the conformational space of the TCR-pMHC complex.

Typically, docking angle (angle between the MHC pocket and the vector between the TCR domains) and incident angle (angle between the MHC peptide groove plane normal vector and the TCR interdomain axis of rotation) are used to describe the orientation of TCR over pMHC. Using these established ones as CVs would enhance clarity.

Answer: We used X and Y as CVs to allow us to account for a wider range of movement, including lateral movement within the plane TCR-pMHC interface. We hypothesized that this type of movement can result from cell movement and play a role in physiological interactions.

2. The justification for applying restraints on the C-alpha atoms of MHC needs to be clarified. How does this approach prevent inappropriate orientations between pMHC and TCR? The authors should explain how these restraints do not limit the sampling of relevant conformations in the TCR-pMHC complex.

Answer: 1000 $[\frac{kJ}{au^2 \times mol}]$, is a soft limit allowing an efficient sampling that includes values up to 35 degrees of TCR tilt. Only C-alpha atoms of the beta-sheet in the MHC were restricted. This accounts for physiological restriction on MHC movement: MHC is anchored in the membrane by a transmembrane domain and is tightly clustered. No restrictions were applied to MHC helixes that are responsible for TCR interaction. Our goal was to focus on peptide-specific physiologically relevant TCR-pMHC interaction at the interface, specifically during the early stages of TCR-pMHC engagement following initial recognition events. TCR-pMHC interactions proceed in the context of constrained space between target and effector cell membranes. Both TCR and pMHC are also present on the surface of the membrane as clusters thus facilitating mostly vertical orientation. This, in turn, limits physiologically relevant TCR tilt from the normal vector to the pMHC surface. According to Singh et al., Proteins. 2019;88:503–513, incidence angles for physiologically derived TCR-pMHC complexes don't exceed ~35 degrees. Based on our analysis, we conclude that our limitations reflect physiological conditions. The tilt angle analysis below was done with the same settings as described for metadynamics simulation in the main methods, except equilibrium trajectories were used for plumed driver routine.

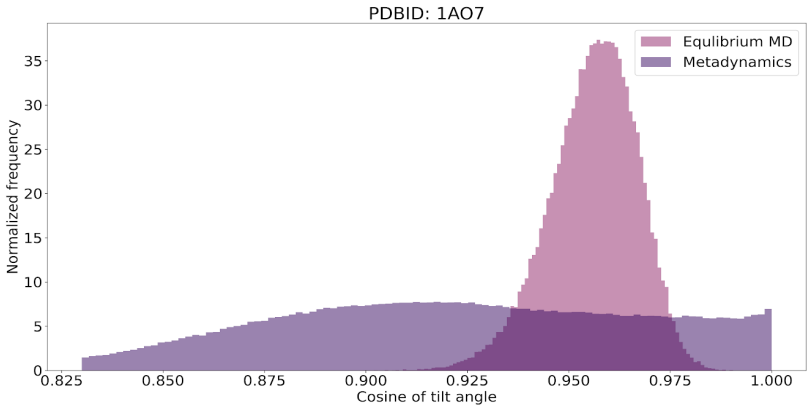

Histogram analysis of values of the tilt angle (scheme on Fig 1) in equilibrium simulation molecular dynamics and in metadynamics simulation of TCR-peptide-MHC binding process.

3. The reason for using two collective variables to explore the metastable states of the complex is unclear. A detailed explanation of how these CVs contribute to understanding metastable states would strengthen the argument.

Answer: We defined X and Y as coordinates on a plane of pMHC surface to allow us to account for lateral movement of the TCR in the plane in addition to TCR turn and tilt. We assume lateral movement can be forced by cell movement and might have a significant contribution to signaling.

4. The authors should consider presenting 1D free energy surfaces for the appropriate collective variables, which will provide more insight into the metastable states and the energy barriers separating them. This will also allow for easier comparison between the stimulatory and non-stimulatory pMHC ligands.

Answer: Please see below 1D RMSD FES.

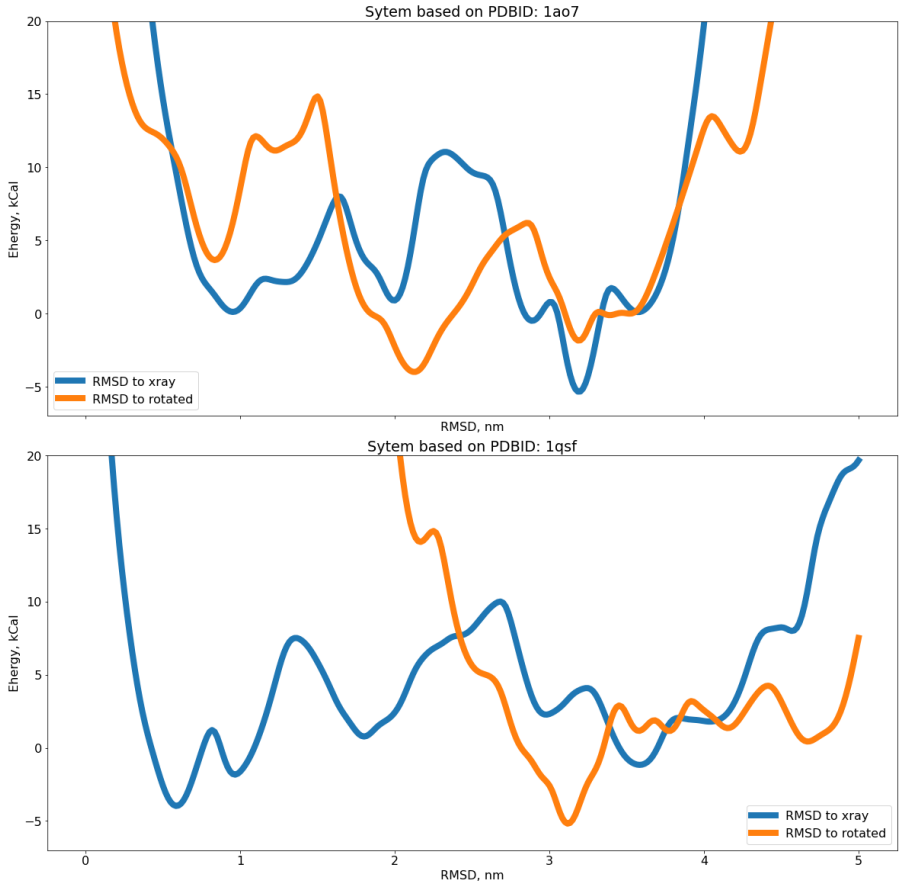

5. The authors should confirm that the free energy surfaces have converged, ensuring the statistical significance and reliability of the results.

Answer: Confirmed that FES converged.Please see supplemental information (picture below)

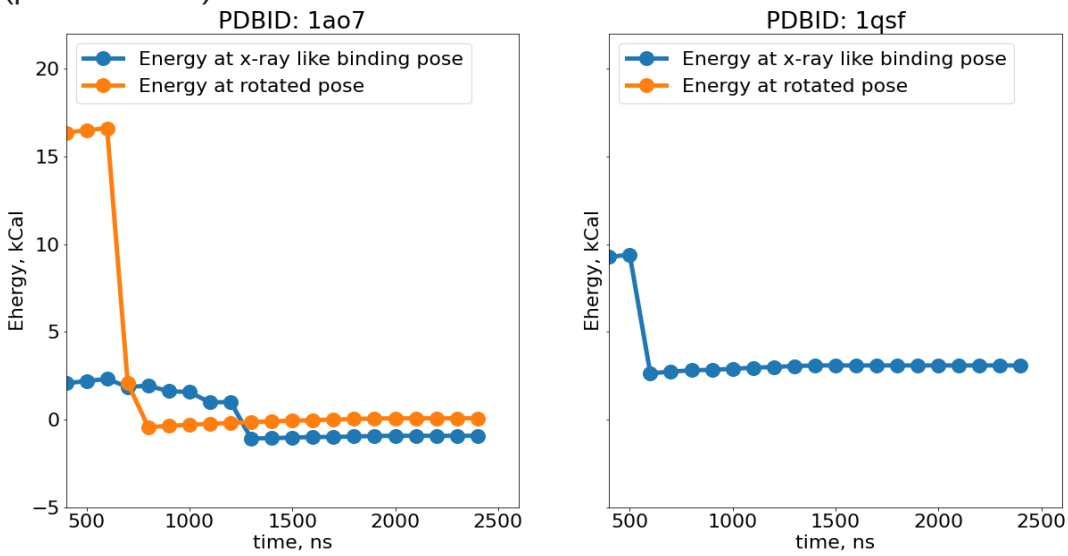

6. None of the figures provided in the manuscript are clear. They are quite blurred, making it difficult to interpret the data. The authors need to replace all the figures with higher-quality versions that are clear and easy to understand.

Answer: all figures have been reproduced with higher quality

The role of peptide conformation presented by MHC in the induction of TCR triggering

Andrey V Golovin[1)], Sergey Panteleev[2)], Alexander S Zlobin[1)], Nadia Anikeeva[2)], Ivan Smirnov[5,6)], Alexander Gabibov[5,6)], and Yuri Sykulev[2,3,4*)]

[1)]School of Bioengineering and Bioinformatics, Lomonosov Moscow State University, Moscow, Russia
Departments of [2)]Microbiology and Immunology and [3)]Medical Oncology and [4)]Sidney Kimmel Cancer Center, Thomas Jefferson University, Philadelphia, USA
[5)]Shemyakin-Ovchinnikov Institute of Bioorganic Chemistry, Russian Academy of Sciences and [6)]Department of Fundamental Medicine, Lomonosov Moscow State University, Moscow, Russia

*Corresponding Author:

Yuri Sykulev
Departments of Microbiology and Immunology
and Medical Oncology
Sidney Kimmel Cancer Center
Thomas Jefferson University
233S 10th St, BLSB 706
Philadelphia, PA 19107

Phone: 215-503-4530
E-mail: Yuri.Sykulev@Jefferson.edu

Running title: Peptide conformation allotment defines TCR triggering

Key words: T-cell receptor-ligand interactions, well-tempered metadynamics and supercomputing, the structure of MHC presented peptides, T-cell receptor triggering

ABSTRACT

High resolution crystal structure of stimulatory peptide-MHC (pMHC) ligands bound to TCR revealed different conformation of the two peptides at positions P6 and V7 compared to the conformation of the same peptides presented by unliganded MHC. Supercomputer simulation and well-tempered metadynamics approach revealed several meta-stable non-canonical TCR-pMHC interactions that depend on the conformation of the MHC-bound peptides. The diversity of meta-stable states was significantly more represented in signaling TCR-pMHC complex. These findings suggest that TCR-pMHC recognition can be informed by a conformation of peptide presented by MHC that notably influences the orientation of TCR recognizing pMHC ligand. It appears that TCR bound to stimulatory pMHC possess a significantly higher degree of freedom to assume various metastable TCR orientations which are distinct from canonical docking. In contrast, TCR interacting with non-stimulatory pMHC ligand revealed markedly less meta-stable non-canonical interactions and disengaged from the pMHC. This suggests that productive TCR-mediated signaling may depend on non-canonical interactions between TCR and pMHC, either facilitating early recognition events or providing new contacts for catch-bond formation. Our discovery can inform future attempts to simulate the catch-bond formation mechanism in TCR-pMHC recognition, allowing the formation of new bonds mediating alternative peptide presentation.

STATEMENT OF SIGNIFICANCE

T-cell receptor (TCR) is a multisubunit complex containing recognition and signaling units. How TCR discriminates between stimulatory and non-stimulatory pMHC ligands is not understood. We have applied well-tempered metadynamics and supercomputing to reveal several meta-stable non-canonical TCR-pMHC interactions that depend on the conformation of MHC-bound peptides. Modeling of various TCR orientations relative to stimulatory pMHCs revealed a unique metastable TCRs orientation bound to stimulatory pMHCs that was not evident for TCRs interacting with non-stimulatory pMHC ligands. This suggests that establishing a unique metastable TCR position relative to pMHC is required for TCR triggering and has not been previously observed.

INTRODUCTION

TCR is a transmembrane multisubunit protein complex that contains α,β-TCR recognition unit and CD3 signaling complex. TCR recognizes binary ligands - short peptide fragments presented by MHC proteins. Both MHC moiety and peptide adduct contribute to TCR-pMHC interactions (1). Relative contributions of the peptide and MHC are not clearly defined, but they are likely varied and depend on TCR, MHC and peptide combination. TCR could also recognize MHC proteins that are not expressed in the host and are called allo-MHC. Although it is believed that allo-MHC moiety contributes significantly more than peptide to the TCR binding (1) and, therefore, could be recognized in association with various self-peptides (2-5), in some cases TCR recognition of allo-MHC is strongly peptide-dependent (6,7). It is likely that peptides could induce a unique conformation of MHC helixes that mediate interactions with the TCR (5,8). It has been shown that TCR can recognize various peptides bound to the MHC, accounting for TCR cross-reactivity. How is TCR capable of recognizing multiple peptide-MHC proteins? Available evidence suggests that the flexibility of TCR CDR loops allows specific binding to the contact surface of various pMHC ligands (9,10). In addition, water molecules that are trapped in the cavities at the TCR-pMHC interface could also contribute to the stability of TCR-pMHC complex (11,12). Variation in relative orientation of pMHC-bound TCR is yet another factor that is thought to influence the specificity of TCR towards various pMHC ligands (13,14).

Because MHC molecules and TCR are confined to the cell surface, the TCR on a T cell recognizes pMHC ligands on the surface of other cells, called antigen presenting or target cells. This makes it very difficult to analyze TCR-pMHC interactions at physiological conditions and to understand molecular basis of antigen recognition by TCR. Since TCR and MHC proteins are not randomly distributed on the cell surface and could form homo and hetero clusters with other cell surface molecules (15-19), evaluation of the TCR-pMHC interactions occurring between the two cells becomes even more complex. In addition, not all TCRs that bind to pMHC with appreciable affinity trigger T cell activation (e.g., (20)). These findings suggest that the mode of TCR engagement by pMHC regulates communications between TCR recognition unit and CD3 signaling complex determining in a large extent mechanism of the induction of TCR-mediated signaling and quality of T cell response (21). In accord with this, a recent discovery shows that

productive TCR engagement is linked to catch bond formation as opposed to non-productive engagement (22,23) . However, the mechanism of catch bond formation is not understood. A recent approach utilizing steered molecular dynamics (SMD) simulations to model the observed conformational changes in TCR and MHC in response to mechanical stress provided evidence suggesting a mechanism of signal initiation and propagation (24). However, the exact mechanism of the catch-bond formation at the interface is not clear and remains to be understood. Indeed, there has been rising interest in utilizing computational approaches to analyze properties of the TCR-pMHC interface that contribute to antigen recognition (25).

We have utilized available data of high-resolution structures of well characterized TCR-pMHC complexes (14,26) and applied supercomputer simulations and well-tempered metadynamics approach that reveal the dynamic changes of TCR-pMHC interactions. We have found that initial TCR engagement resulting in establishing canonical orientation of pMHC-bound TCR may change allowing formation of various metastable positions. One of such positions may be unique for TCR bound to stimulatory but not to non-stimulatory pMHC. These data provide a novel insight into how dynamic changes at the TCR-pMHC interface influence antigen recognition by TCR and triggering TCR-mediated signaling.

RESULTS

Approach

Having the structure of the TCR-pMHC interface at high resolution, we exploited an approach that allows to model dynamics of TCR-pMHC interactions and to identify various TCR orientations over the stimulatory and non-stimulatory pMHC ligands. Because the binding of TCR to pMHC occurs at the interface between the two cells, it is expected that the interaction between cell surface proteins is limited by deviations from the initial contact between the two cells. For both receptor and ligand, their orientation is further constrained by TCR and MHC clustering (27),(28). Thus, the physiological range of possible angles of TCR-pMHC interaction that are peptide-specific is limited (29). Based on these considerations, we introduced restraints in our modeling to impose positional restrictions on the C_a atoms in the beta-sheets of MHC molecule to avoid inappropriate orientations between interacting pMHC ligands and TCRs (**Fig. 1**). To identify possible interactions between the TCR loops and the peptide-MHC surface, we

exploited metadynamics, a variant of biased molecular dynamics that allows faster scanning of conformational space for complex systems in a time-dependent manner. We maintain freedom of the TCR movement relative to the surface of the pMHC while imposing restrictions on the TCR displacement from the surface of the pMHC, keeping a generally vertical TCR orientation (**Fig. 1**). Movements over the surface of the pMHC were also limited to minimize the time the proteins spent in an unbound state. Thus, while maintaining the position of the MHC, it was possible to test multiple probing of the pMHC surface by TCR, allowing the mobility of atoms in both TCR and pMHC interacting surfaces.

Static crystal structures fail to divulge the mechanism of antigen recognition by TCR.

To model the dynamic behavior of TCR bound to either stimulatory or non-stimulatory pMHC ligands, we utilized available high-resolution TCR-pMHC crystal structures of A6-TAX-HLA-A2 and A6-Y8A-HLA-A2 complexes (1ao7 and 1qsf in PDB)(30). The stimulatory complex TAX-HLA-A2 is recognized by A6 TCR and differs from the non-stimulatory complex by one amino-acid residue in the TAX peptide (Y8A) (**Figure 2A, B**). The two X-ray structures were found to be almost identical, except for a possible hydrogen bond between β-CDR1 and Y8 in the TAX peptide (**Figure 2C, Supplementary Figure 1 and 2**). The lack of significant difference in crystal structure between stimulatory and non-stimulatory TCR-pMHC complexes suggested that the TCR is capable of distinguishing ligands based on the dynamic properties of the contact interfaces. To reveal these properties, we resorted to well-tempered meta-dynamic simulations.

The meta-dynamics approach reveals unique intermediary states in cognate antigen recognition.

We started from 6 different non-X-ray states, and the full atomic model simulation revealed the canonical orientations as well as metastable intermediate states of both signaling (A6-TAX-HLA-A2) and non-signaling A6-Y8A-HLA-A2 TCR-pMHC complexes. This analysis was also performed independently of available information on the crystal structure of the TCR-pMHC complexes and reproduced both canonical and metastable states of TCR orientation. Our initial analysis of simulated TCR-pMHC complexes allowed us to compare the torsion angles of TCR relative to both pMHCs and revealed a unique metastable state in the stimulatory A6-TAX-HLA-A2 complex (**Figure 3 and Supplemental Figure 3-4**). To overcome the

limitations of the histogram analysis by TCR torsion angle, we exploited a more accurate approach of Root Mean Square Deviation (RMSD) for both X-ray structures and found the unique metastable state in the signaling complex (**Figure 4 and Supplemental Figures 5-6)** This analysis reveals the stark contrast between stimulatory and non-stimulatory complexes, demonstrating that non-stimulating complex A6-Y8A-HLA-A2 lacks the degrees of freedom to assume metastable states that are observed in the stimulatory complex.

Signaling complex archives unique intermediary states during antigen recognition via conformational changes in peptide presentation.

In a metastable state of the A6-TAX-HLA-A2 signaling complex, the TCR adopted a "reversed orientation", i.e., 171.6 degree turn around TCR-pMHC interface central axis that is positioned near Y5 of the peptide (**Fig. 3a,b**). This conformation appears to be an intermediary state of the complex during initial pMHC recognition by TCR. The new TCR orientation has been achieved through a different mode of peptide presentation (**Figure 5A**). While structures of TAX and mutated Y8A peptides within the HLA-A2 binding grove of the canonical TCR-pMHC complexes were identical with the exception of the presence of tyrosine in position 8, the C-terminal end of the peptide bound to TCR in reverse orientation experiences significant changes of its conformation accompanied by a change in special arrangements of the MHC helixes (**Fig. 5 a,b**). Specifically, the close positioning of **Y5** and **Y8** within the peptide results in a very different landscape of the pMHC contact surface. This re-arrangement is facilitated by the conformational change of the peptide backbone, with **V7** facing the MHC binding groove similar to peptide conformation found in TAX-MHC crystal complex (**Supplemental Figure 7**). This conformational change is facilitated by a "kink" in the alpha-1 helix, which creates new contacts between His70 and His74 of the alpha-1 helix and backbone oxygen of V7 (**Figure 5C**). These redundant hydrogen bonds facilitate the novel peptide-MHC conformation, establishing non-canonical TCR orientation (**Fig. 5A-C**).

The allogeneic TCR-pMHC complex assumes intermediate states resembling those found in the non-signaling syngeneic complex.

We applied the same approach to analyze the dynamic behavior of TCR in two allogeneic TCR-pMHC complexes, namely, signaling (42f3-QL9-H2-L^d) and high affinity non-signaling non-canonical (42f3-p3A1-H2-L^d) complexes (**Fig. 6**).

Initial analysis of the TCR torsion angle relative to the pMHC revealed that neither signaling nor non-signaling 42f3-QL9/p3A1-H2-L^d complexes had any significant free-energy minima similar to the unique metastable state in A6-TAX-HLA-A2 complex (**Supplemental Fig. 4**). A low affinity (K_d ~399 mM) (14) of signaling allogenic complex 42f3-QL9 -H2-L^d has all its significant free-energy minima located at torsion angles resembling X-ray structure (**Fig 6 and Supplemental Fig 4**). Non-signaling high-affinity system with synthetic peptide 42f3-p3A1-H2-L^d (K_d ~3.9 mM) also has its significant minima resembling the X-ray structure, a unique non-canonical structure reported in (14) (**Fig 6 and Supplemental Fig 4**). Importantly, the Free Energy Surface maps of non-signaling complex A6-Y8A-HLA-A2 revealed the deepest minima at a torsion angle that is similar to the minima found in both low-affinity signaling 42f3-QL9-H2-L^d complex and high affinity non-signaling 42f3-p3A1-H2-L^d complex (**Supplemental Figure 4 and 8**). These data suggest that some TCR orientations don't facilitate effective TCR triggering and signaling.

The allogeneic system lacks the required degrees of freedom to assume intermediate states found in syngeneic signaling complex.

To effectively compare syngeneic and allogenic systems we performed RMSD calculations for the second system. This approach requires reference structures, in this case, X-ray, and unique metastable orientation found in A6-TAX-HLA-A2. Since the simulations of the second allogeneic system did not reveal any significant unique metastable states, we had to use rare conformations approximating the unique metastable orientation found in the A6-TAX-HLA-A2 metastable state (**Fig. 7**). This analysis confirmed that both low-affinity signaling 42f3-QL9-H2-L^d complex and high-affinity non-singling 42f3-p3A1-H2-L^d complex lack the degree of freedom necessary to assume conformations similar to the unique metastable state found in A6-TAX-HLA-A2 (**Fig. 8**). A notable limitation of this analysis is the loss of accuracy with increasing RMSD values, resulting in heterogeneous clustering. Thus, we observe heterogeneous deep minima for both systems at extreme torsion angles and high RMSD values.

DISCUSSION

Our findings demonstrate that analysis of possible dynamic variations of TCR positioning bound to pMHC allowed to identify differences in metastable TCR orientations for stimulatory and non-stimulatory pMHC ligands. These data let us identify a metadynamic state of TCR orientation that was evident only for the stimulatory TCR-pMHC complexes but not for non-stimulatory complexes, suggesting that this unique TCR orientation makes a critical contribution to antigen recognition and TCR triggering.

It is notable that MHC-bound peptides that play essential role in determining the specificity of TCR-pMHC interactions, has only 20-30% of exposure of the surface area to solvent with the rest being buried in the MHC binding groove (31). Assuming that on average 25 cal per $Å^2$ can be contributed for protein-protein interactions, the peptide contribution would be limited to 3,500 cal, while the free energy (ΔG^O) of TCR-pMHC interactions may vary from 6,000 to 9,700 cal (1). Thus, MHC moiety supplies a comparable or significantly larger amount of energy stabilizing TCR-pMHC complex. This suggests that TCR recognizes not only the specific peptide presented by self-MHC but rather the whole p-MHC interface. Indeed, peptide binding could change the conformation of MHC helixes (32), which is further altered by the emergence of MHC extended conformations resulting from mechanical stress facilitated by TCR-pMHC catch bond formation (33) that contribute to the specificity of TCR towards pMHC ligand. Despite a relatively small accessible surface, MHC-bound peptide significantly influences the landscape of the pMHC contact surface and interactions of MHC helixes with TCR. Thus, the peptide could either directly or indirectly mediate the specificity of TCR-pMHC reactions (5,9,34). For example, the formation of A6-TAX-HLA-A2 complex results in changes in TAX peptide conformation at positions at P6 and V7 (26). The same residues experience further conformational changes facilitating alternative TCR orientations (see **Fig**. **4** and **Supplemental Figure 7**). The above considerations regarding the peptide contribution to the specificity of TCR-pMHC suggest that initial pMHC binding to TCR may not mediate TCR triggering. Subsequent dynamic changes of the TCR orientation over pMHC surface and the formation of a unique metastable TCR positioning over pMHC appear to be a hallmark of productive TCR engagement. Under these circumstances, TCR CDR interactions with agonist pMHC-ligand, but not null pMHC, mediate the formation of metastable TCR-pMHC complex required for TCR triggering. Thus, our findings suggest that

previously “invisible” peptide contribution may influence pMHC landscape and TCR orientation over various pMHC ligands. Indeed, in the crystal structures of TCR-pMHC complexes analyzed here (14,26) the formation of metastable TCR orientation relative to stimulatory and non-stimulatory peptide-pMHC complexes were observed and provide further evidence that a unique TCR orientation relative to pMHC constitutes the mechanism by which TCR discriminates between various peptides bound to the same MHC. These data may suggest that the “reverse orientation” of TCR over pMHC might stunt signaling due to inefficient Lck ITAM phosphorylation caused by spatial constraints of CD8 binding (35). However, recently reported mechanical properties of the TCR, namely its ability to assume an extended conformation under mechanical stress (23) suggest that a productive syngeneic recognition event might not have these limitations. It is plausible that the mechanically induced TCR conformational changes could relieve any spatial constraints precluding CD8 from delivering Lck close enough to the ITAM CD3 complex. Namely, taking advantage of the CD8 extracellular domain’s capacity to stretch along extended TCR in order to remain in contact with the α3-MHC domain.

It is very likely that unique metastable TCR orientation over the stimulatory pMHC leads to formation of a stronger TCR-pMHC interactions. It has been shown that T-cells during scanning target cells hunting for antigen apply tension to TCR-pMHC complexes within observed permissive ranges of force, i.e., 10-20 pN (23,24). This may lead to alternative thermodynamically favorable TCR-pMHC orientations, allowing the formation of new bonds under stress, i.e., the formation of catch bonds. Indeed, the formation of a strong TCR-pMHC interaction under shear force was observed in experiments utilizing biomembrane force probe and was defined as catch bond (22). However, it was not clear whether the formation of the catch bonds requires strengthening of preexisting bonds or the formation of new bonds under mechanical stress. Indeed, recognition of non-stimulatory peptide-MHC ligands leads to the formation of slip bonds and rapid TCR-pMHC dissociation. Ellis Reinherz and colleagues have used the laser trap to apply force to the TCR-pMHC bond in either cell free system or the system with live T cells and also demonstrated the formation of catch and slip bounds (23). In addition, they have proposed that FG loop at the C-terminal end of the TCR β-chain play an important role in the formation of catch bond. Demonstration of catch and

slip bonds provides basis to link the formation of these bonds to our findings suggesting mechanism by which engaged α,β-TCR "informs" CD3 complex to initiate signaling.

Based on the above considerations, we would like to propose that TCR recognition is based on distinguishing between various landscape patterns of pMHC contact surface that are mediated by MHC-bound peptide. Our findings have important implication for designing TCR that could be optimally engaged by pMHC of interest after virtual maturation of TCR-pMHC interface to achieve the most favorable energy distribution at the interface. An optimal TCRs could then be utilized to engineer highly effective T cells for therapeutic interventions to fight viruses and cancer.

Methods

Model building

MHC-peptide-TCR complex models were built from PDB ID: 1ao7, 1qsf, 3tf7, and 3tjh. For each model, only Fv fragments of TCR and MHC contact surface (residues 1-180) were utilized. For all models, the contact MHC surface was positioned along the XY plane of the simulation.

MM Model Preparation and Equilibration

All models listed above were parameterized in the Amber99sb force field (33). Each structure was placed in a cubic box with periodic boundary conditions and solvated with TIP3P (36). Na^+ and Cl^- ions were added to neutralize the net charge and reach 0.15 M ionic strength. Modeling of each structure was minimized to 5000 steps of the steepest descent. All simulations were performed at T = 300 K with a velocity rescaling thermostat (34) for temperature coupling, and a stochastic cell-rescaling barostat was used for pressure control (35). A time step of 2 fs was used in all systems under study. Coulomb interactions were evaluated with particle mesh Ewald method (37) for long-range electrostatics interactions (PME) with short and long-range cutoff radius 0.9nm and the same cutoff radius for VdW interaction.

System setup

The interaction of TCR with pMHC occurs between the two cells; it is expected that this contact is limited due to deviations from the membrane surface (**Figure 1**). We implemented this consideration in the form of a restraint in our modeling of the deviations of the pMHC from the normal vector to the cell surface when imposing positional restrictions of 100 kJ/mol on the C-alpha atoms of the beta sheet in the MHC. The mostly vertical orientation of TCR relative to MHC was maintained with PLUMED's (38) lower wall restraining bias on vector projection to normal MHC position at the cell surface (**Fig. 1**). Vector was defined with two points: center of mass (COM) for TCR loops to the center of mass of the whole TCR. The restrain was positioned at 0.82 with force constants 1000 [$\frac{kJ}{au^2 \times mol}$], which corresponds to an angle of about 35 degrees.

To effectively scan possible interactions between the TCR loops and the MHC surface with the presented peptide, we utilized well-tempered metadynamics in Gromacs (36) with the Plumed plugin where we used two collective variables X and Y coordinates of TCR Center Of Mass interacting with the pMHC surface that defines the XY plane. Well-tempered metadynamics is a variant of molecular dynamics with imposed time-dependent bias. The freedom of movement of the TCR over the pMHC surface was maintained while imposing restrictions on displacement beyond the surface of the pMHC and maintaining a generally vertical orientation as described above. The allowed XY TCR Center of Mass (COM) coordinates were restrained with elliptical cylinder potential oriented to the normal of MHC surface with a-radius 5 nm and b-radius 5.5 nm. Movement along the normal vector to the pMHC surface was also limited with an upper wall restraint on TCR COM position at 5.8 nm on the normal vector, minimizing the time that proteins spent in an unbound state. Thus, while maintaining the position of the MHC, it was possible to carry out multiple probing of the pMHC surface by TCR, including the mobility of atoms in both proteins and the peptide.

Exploration runs

Each exploration run with metadynamics was performed with a 1 μs simulation length. Well-tempered metadynamics simulations were performed for each of the four initially bound TCR-pMHC models. The

Gaussian potential with a height of 1 kJ/mol and a width of 0.05 nm was deposited every 500 steps. The bias factor was set to 16. (**Supplemental Figure 3**)

Production runs

We selected six minima on free energy surface and used them as starting points for the production run with six walkers. Each of the six walker runs had a trajectory length of 2.5 μs with a 2-fs time step resulting in a 15 μs metadynamics trajectory length for every system. Aggregate information from the walkers was used to assess and confirm the convergence of simulations for each individual starting model. Aggregate information between different starting models was used to assess and confirm reproducibility and build final free energy profiles. In each scenario, Tiwary reweighting (39) was used to build profiles with the first 500 ns of a walker run discarded as the initial transient. The same scheme was utilized later to project profiles to different variables.

Supplementary Methods.

Convergence analysis. Metadynamics simulation was done in six walkers. For each walker, we saved the c(t) reweighting factor and used that to obtain the normalized bias. Thus, all data from walkers were joined to a new file with the pandas module in Python. With the selected trajectory time slice we saved separate files and used them to estimate FES at a certain time in all walkers with the above-mentioned reweighting procedure.

H-bond analysis. We used equilibrium molecular dynamics simulation as a reference for biased dynamics to estimate the h-bond lifetime. Hydrogen bond between β-CDR1 and Y8 of the TAX peptide were analysed with the MDAnalysis module for Python (40) as described in documentation.

Author Contributions

YS, AG, AVG, IS proposed experimental design and expected outcomes; AVG, ASZ, SP work on simulation design, supercomputing; AVG, SP, NA, YS analysis of the results and graphic design; YS, AVG, SP, NA, AG, IS concept formulation, discussion and manuscript writing.

The authors declare no competing interests. All authors indicated that they don't have financial or other interests related to studies described in the manuscript.

ACKNOWLEDGMENTS - This work was supported by CA217714 grant from NIH and RFBR-NIH #17-54-30025 grants to Y.S. and I.S.; and by the Russian Science Foundation grant #21-74-20113 to AG and AS. The supercomputer simulations were carried out using the equipment of the shared research facilities of HPC computing resources at Lomonosov Moscow State University.

References

1. Eisen, H. N., Y. Sykulev, and T. J. Tsomides. 1997. The antigen-specific T-cell receptor and its reactions with peptide-MHC complexes. In Adv. Prot. Chem., Antigen-Binding Molecules: Antibodies and T-cell Receptors. E. Haber, editor. Academic Press, San Diego, pp. 1-56.
2. Elliott, T. J., and H. N. Eisen. 1990. Cytotoxic T lymphocytes recognize a reconstituted class I histocompatibility antigen (HLA-A2) as an allogeneic target molecule. *Proc. Natl. Acad. Sci. USA*. 87:5213-5217.
3. Rötzschke, O., K. Falk, S. Faath, and H.-G. Rammensee. 1991b. On the nature of peptides involved in T cell alloreactivity. *J. Exp. Med.* 174:1059-1071.
4. Brock, R., K. H. Wiesmuller, G. Jung, and P. Walden. 1996. Molecular basis for the recognition of two structurally different major histocompatibility complex/peptide complexes by a single T-cell receptor. *Proc Natl Acad Sci U S A*. 93(23):13108-13113, http://www.ncbi.nlm.nih.gov/entrez/query.fcgi?cmd=Retrieve&db=PubMed&dopt=Citation&list_uids=8917552.
5. Daniel, C., S. Horvath, and P. M. Allen. 1998. A basis for alloreactivity: MHC helical residues broaden peptide recognition by the TCR. *Immunity*. 8(5):543-552, doi: 10.1016/s1074-7613(00)80559-2, https://www.ncbi.nlm.nih.gov/pubmed/9620675.
6. Udaka, K., T. J. Tsomides, and H. N. Eisen. 1992. A naturally occurring peptide recognized by alloreactive $CD8^+$ cytotoxic T lymphocytes in association with a class I MHC protein. *Cell*. 69:989-998.
7. Connolly, J. M. 1994. The peptide p2Ca is immunodominant in allorecognition of Ld by beta chain variable region V beta 8+ but not V beta 8- strains. *Proc Natl Acad Sci U S A*. 91(24):11482-11486, doi: 10.1073/pnas.91.24.11482, https://www.ncbi.nlm.nih.gov/pubmed/7972088.
8. Alexander-Miller, M., R. A. Robinson, J. D. Smith, W. E. Gillander, L. Harrison, T. H. Hansen, J. M. Connoly, and D. R. Lee. 1994. Defenition of TCR recognition sites on Ld-tum-complexes. *Int. Immunol.* 6:1699.
9. Borbulevych, O. Y., K. H. Piepenbrink, B. E. Gloor, D. R. Scott, R. F. Sommese, D. K. Cole, A. K. Sewell, and B. M. Baker. 2009. T cell receptor cross-reactivity directed by antigen-dependent tuning of peptide-MHC molecular flexibility. *Immunity*. 31(6):885-896, doi: 10.1016/j.immuni.2009.11.003, https://www.ncbi.nlm.nih.gov/pubmed/20064447.
10. Ayres, C. M., D. R. Scott, S. A. Corcelli, and B. M. Baker. 2016. Differential utilization of binding loop flexibility in T cell receptor ligand selection and cross-reactivity. *Sci Rep*. 6:25070, doi: 10.1038/srep25070, https://www.ncbi.nlm.nih.gov/pubmed/27118724.
11. Anikeeva, N., T. Lebedeva, M. Krogsgaard, S. Y. Tetin, E. Martinez-Hackert, S. A. Kalams, M. M. Davis, and Y. Sykulev. 2003a. Distinct molecular mechanisms account for the specificity of two different T-cell receptors. *Biochemistry*. 42:4709-4716.
12. Stewart-Jones, G. B., A. J. McMichael, J. I. Bell, D. I. Stuart, and E. Y. Jones. 2003. A structural basis for immunodominant human T cell receptor recognition. *Nat. Immunol.* 4(7):657-663.
13. Gras, S., J. Chadderton, C. M. Del Campo, C. Farenc, F. Wiede, T. M. Josephs, X. Y. X. Sng, M. Mirams, K. A. Watson, T. Tiganis, K. M. Quinn, J. Rossjohn, and N. L. La Gruta. 2016. Reversed T Cell Receptor Docking on a Major Histocompatibility Class I Complex Limits Involvement in the Immune Response. *Immunity*. 45(4):749-760, doi: 10.1016/j.immuni.2016.09.007, https://www.ncbi.nlm.nih.gov/pubmed/27717799.

14. Adams, J. J., S. Narayanan, B. Liu, M. E. Birnbaum, A. C. Kruse, N. A. Bowerman, W. Chen, A. M. Levin, J. M. Connolly, C. Zhu, D. M. Kranz, and K. C. Garcia. 2011. T cell receptor signaling is limited by docking geometry to peptide-major histocompatibility complex. *Immunity*. 35(5):681-693, doi: 10.1016/j.immuni.2011.09.013, https://www.ncbi.nlm.nih.gov/pubmed/22101157.
15. Hwang, J., L. A. Gheber, L. Margolis, and M. Edidin. 1998. Domains in cell plasma membranes investigated by near-field scanning optical microscopy. *Biophys J*. 74(5):2184-2190, doi: S0006-3495(98)77927-5 [pii]10.1016/S0006-3495(98)77927-5, http://www.ncbi.nlm.nih.gov/entrez/query.fcgi?cmd=Retrieve&db=PubMed&dopt=Citation&list_uids=9591645.
16. Lebedeva, T., N. Anikeeva, S. A. Kalams, B. D. Walker, I. Gaidarov, J. H. Keen, and Y. Sykulev. 2004. Major histocompatibility complex class I-intercellular adhesion molecule-1 association on the surface of target cells: implications for antigen presentation to cytotoxic T lymphocytes. *Immunology*. 113(4):460-471, http://www.ncbi.nlm.nih.gov/entrez/query.fcgi?cmd=Retrieve&db=PubMed&dopt=Citation&list_uids=15554924.
17. Zhong, L., G. Zeng, X. Lu, R. C. Wang, G. Gong, L. Yan, D. Huang, and Z. W. Chen. 2009. NSOM/QD-based direct visualization of CD3-induced and CD28-enhanced nanospatial coclustering of TCR and coreceptor in nanodomains in T cell activation. *PLoS One*. 4(6):e5945, doi: 10.1371/journal.pone.0005945, http://www.ncbi.nlm.nih.gov/entrez/query.fcgi?cmd=Retrieve&db=PubMed&dopt=Citation&list_uids=19536289.
18. Ferez, M., M. Castro, B. Alarcon, and H. M. van Santen. 2014. Cognate peptide-MHC complexes are expressed as tightly apposed nanoclusters in virus-infected cells to allow TCR crosslinking. *J Immunol*. 192(1):52-58, doi: 10.4049/jimmunol.1301224, https://www.ncbi.nlm.nih.gov/pubmed/24307729.
19. Anikeeva, N., N. O. Fischer, C. D. Blanchette, and Y. Sykulev. 2019. Extent of MHC Clustering Regulates Selectivity and Effectiveness of T Cell Responses. *J Immunol*. 202(2):591-597, doi: 10.4049/jimmunol.1801196, https://www.ncbi.nlm.nih.gov/pubmed/30541879.
20. Al-Ramadi, B. K., M. T. Jelonek, L. F. Boyd, D. H. Margulies, and A. L. Bothwell. 1995. Lack of strick correlation of functional sensitization with the apparent affinity of MHC/peptide complexes for the TCR. *J. Immunol.* 155:662-673.
21. Gil, D., W. W. Schamel, M. Montoya, F. Sanchez-Madrid, and B. Alarcon. 2002. Recruitment of Nck by CD3 epsilon reveals a ligand-induced conformational change essential for T cell receptor signaling and synapse formation. *Cell*. 109(7):901-912, doi: S0092867402007997 [pii], http://www.ncbi.nlm.nih.gov/entrez/query.fcgi?cmd=Retrieve&db=PubMed&dopt=Citation&list_uids=12110186.
22. Liu, B., W. Chen, B. D. Evavold, and C. Zhu. 2014. Accumulation of dynamic catch bonds between TCR and agonist peptide-MHC triggers T cell signaling. *Cell*. 157(2):357-368, doi: 10.1016/j.cell.2014.02.053, https://www.ncbi.nlm.nih.gov/pubmed/24725404.
23. Das, D. K., Y. Feng, R. J. Mallis, X. Li, D. B. Keskin, R. E. Hussey, S. K. Brady, J. H. Wang, G. Wagner, E. L. Reinherz, and M. J. Lang. 2015. Force-dependent transition in the T-cell receptor beta-subunit allosterically regulates peptide discrimination and pMHC bond lifetime. *Proc Natl Acad Sci U S A*. 112(5):1517-1522, doi: 10.1073/pnas.1424829112, https://www.ncbi.nlm.nih.gov/pubmed/25605925.

24. Choi, H. K., P. Cong, C. Ge, A. Natarajan, B. Liu, Y. Zhang, K. Li, M. N. Rushdi, W. Chen, J. Lou, M. Krogsgaard, and C. Zhu. 2023. Catch bond models may explain how force amplifies TCR signaling and antigen discrimination. *Nat Commun*. 14(1):2616, doi: 10.1038/s41467-023-38267-1, https://www.ncbi.nlm.nih.gov/pubmed/37147290.
25. Ayres, C. M., S. A. Corcelli, and B. M. Baker. 2023. The Energetic Landscape of Catch Bonds in TCR Interfaces. *J Immunol*. 211(3):325-332, doi: 10.4049/jimmunol.2300121, https://www.ncbi.nlm.nih.gov/pubmed/37459192.
26. Ding, Y. H., B. M. Baker, D. N. Garboczi, W. E. Biddison, and D. C. Wiley. 1999. Four A6-TCR/peptide/HLA-A2 structures that generate very different T cell signals are nearly identical. *Immunity*. 11(1):45-56.
27. Colbert, J. D., F. M. Cruz, C. E. Baer, and K. L. Rock. 2022. Tetraspanin-5-mediated MHC class I clustering is required for optimal CD8 T cell activation. *Proc Natl Acad Sci U S A*. 119(42):e2122188119, doi: 10.1073/pnas.2122188119, https://www.ncbi.nlm.nih.gov/pubmed/36215490.
28. Al-Aghbar, M. A., A. K. Jainarayanan, M. L. Dustin, and S. R. Roffler. 2022. The interplay between membrane topology and mechanical forces in regulating T cell receptor activity. *Commun Biol*. 5(1):40, doi: 10.1038/s42003-021-02995-1, https://www.ncbi.nlm.nih.gov/pubmed/35017678.
29. Singh, N. K., E. T. Abualrous, C. M. Ayres, F. Noe, R. Gowthaman, B. G. Pierce, and B. M. Baker. 2020. Geometrical characterization of T cell receptor binding modes reveals class-specific binding to maximize access to antigen. *Proteins*. 88(3):503-513, doi: 10.1002/prot.25829, https://www.ncbi.nlm.nih.gov/pubmed/31589793.
30. Garboczi, D. N., P. Ghosh, U. Utz, Q. R. Fan, W. E. Biddison, and D. C. Wiley. 1996. Structure of the complex between human T-cell receptor, viral peptide and HLA-A2. *Nature*. 384:134-141.
31. Rudolph, M. G., R. L. Stanfield, and I. A. Wilson. 2006. How TCRs bind MHCs, peptides, and coreceptors. *Annu Rev Immunol*. 24:419-466, http://www.ncbi.nlm.nih.gov/entrez/query.fcgi?cmd=Retrieve&db=PubMed&dopt=Citation&list_uids=16551255
32. Ayres, C. M., S. A. Corcelli, and B. M. Baker. 2017. Peptide and Peptide-Dependent Motions in MHC Proteins: Immunological Implications and Biophysical Underpinnings. *Front Immunol*. 8:935, doi: 10.3389/fimmu.2017.00935, https://www.ncbi.nlm.nih.gov/pubmed/28824655.
33. Wu, P., T. Zhang, B. Liu, P. Fei, L. Cui, R. Qin, H. Zhu, D. Yao, R. J. Martinez, W. Hu, C. An, Y. Zhang, J. Liu, J. Shi, J. Fan, W. Yin, J. Sun, C. Zhou, X. Zeng, C. Xu, J. Wang, B. D. Evavold, C. Zhu, W. Chen, and J. Lou. 2019. Mechano-regulation of Peptide-MHC Class I Conformations Determines TCR Antigen Recognition. *Mol Cell*. 73(5):1015-1027 e1017, doi: 10.1016/j.molcel.2018.12.018, https://www.ncbi.nlm.nih.gov/pubmed/30711376.
34. Mareeva, T., E. Martinez-Hackert, and Y. Sykulev. 2008. How a T cell receptor-like antibody recognizes major histocompatibility complex-bound peptide. *J Biol Chem*. 283(43):29053-29059, doi: M804996200 [pii]
10.1074/jbc.M804996200, http://www.ncbi.nlm.nih.gov/entrez/query.fcgi?cmd=Retrieve&db=PubMed&dopt=Citation&list_uids=18703505.
35. Zareie, P., C. Szeto, C. Farenc, S. D. Gunasinghe, E. M. Kolawole, A. Nguyen, C. Blyth, X. Y. X. Sng, J. Li, C. M. Jones, A. J. Fulcher, J. R. Jacobs, Q. Wei, L. Wojciech, J. Petersen, N. R. J. Gascoigne, B. D. Evavold, K. Gaus, S. Gras, J. Rossjohn, and N. L. La Gruta. 2021. Canonical T

cell receptor docking on peptide-MHC is essential for T cell signaling. *Science*. 372(6546), doi: 10.1126/science.abe9124, https://www.ncbi.nlm.nih.gov/pubmed/34083463.
36. Price, D. J., and C. L. Brooks, 3rd. 2004. A modified TIP3P water potential for simulation with Ewald summation. *J Chem Phys*. 121(20):10096-10103, doi: 10.1063/1.1808117, https://www.ncbi.nlm.nih.gov/pubmed/15549884.
37. Darden, T., D. York, and L. Pedersen. 1998. Particle mesh Ewald: An N·log(N) method for Ewald sums in large systems. *J. Phys. Chem.* 98:10089.
38. Botomi, M., G. Bussi, and C. Camilloni. 2019. Promoting transparency and reproducibility in enhanced molecular simulations. *Nature Methods*. 16:667-673.
39. Tiwary, P., and M. Parrinello. 2015. A time-independent free energy estimator for metadynamics. *J Phys Chem B*. 119(3):736-742, doi: 10.1021/jp504920s, https://www.ncbi.nlm.nih.gov/pubmed/25046020.
40. Beckstein, O., E. J. Denning, J. R. Perilla, and T. B. Woolf. 2009. Zipping and unzipping of adenylate kinase: atomistic insights into the ensemble of open<-->closed transitions. *J Mol Biol*. 394(1):160-176, doi: 10.1016/j.jmb.2009.09.009, https://www.ncbi.nlm.nih.gov/pubmed/19751742.

FIGURE LEGENDS

Figure 1. Model restrictions

To allow sufficient freedom of movement for peptide and TCR while limiting the amount of physiologically irrelevant structures, we restricted the complex volume and TCR tilt while allowing TCR lateral movement. We assume the interaction of TCR and MHC during cell-to-cell contact (A) and that the ligand and receptor are constrained by clustering (B). We defined the volume as cylindrical space around the TCR-pMHC complex and the tilt as a vector connecting TCR and TCR-pMHC centers of mass projected onto the normal vector to the MHC surface (C). The target cell and target cell membrane are red, T-cell and T-cell membrane are blue. TCR is green, MHC helixes is pink, and MHC groove is blue. The cylinder limiting TCR-pMHC space is dark red. The normal vector to the MHC surface is in dark blue. The vector connecting TCR-pMHC and TCR centers of mass is in red.

Figure 2. Positioning of TAX (left) and Y8A (right) Peptides within A6-HLA-A2 complex.

Comparison of A6-TAX-HLA-A2 and A6-Y8A-HLA-A2 complexes represent a rare example of X-ray structures of stimulatory and non-stimulatory TCR-pMHC complexes whose structures are almost identical.

A) X-ray Structure of Stimulatory A6-TAX-HLA-A2 Complex (left) and non-stimulatory A6-Y8A-HLA-A2 complex (right).

B) Peptide Close–up: Differences in peptide conformation in signaling (left) and non-signaling (right) TCR-pMHC complexes.

C) TCR CDRs- X-ray of Stimulatory (left) A6-TAX-HLA-A2 vs non-stimulatory (right) A6-Y8A-HLA-A2. The red box shows the difference in β-CDR-1 contact with Y8 of TAX and A8 of Y8A peptide.

TCR surface is shown as transparent; the peptide backbone is grey, backbone nitrogen is dark blue, oxygen is red, Y8 is cyan, and mutated Y8A is orange. CDRs are shown as: α-CDR-1 is green, α-CDR-2 is purple, α-CDR-3 is dark red, β-CDR-1 is yellow, β-CDR-2 is blue, β-CDR-3 is red.

Figure 3. Meta-dynamics simulation reveals a unique metastable state in the A6-TAX-HLA-A2 signaling complex that is absent in non-signaling A6-Y8A-HLA-A2 complex.

Structure of canonical A6-TAX-HLA-A2 (left) and unique metastable state of A6-TAX-HLA-A2 (right) complexes. In the unique metastable state TCR rotates 171.6 degrees over the MHC surface. TCR surface is shown as transparent, CDRs are shown as α-CDR-1 is green, α-CDR-2 is purple, α-CDR-3 is dark red, β-CDR-1 is yellow, β-CDR-2 is blue, β-CDR-3 is red.

Figure 4. Free Energy Maps of simulated complexes in RMSD and TCR torsion angle coordinates.

A) A6-TAX-HLA-A2 X-ray structure

B) Free Energy Map of A6-TAX-HLA-A2 structure in RMSD and TCR torsion angle coordinates

C) Free Energy Map in RMSD of the simulated unique metastable state structure of A6-TAX-HLA-A2 and TCR torsion angle coordinates

D) A6-TAX-HLA-A2 simulated structure showing the unique metastable state

E) A6-Y8A-HLA-A2 X-ray structure

F) Free Energy Map of A6-Y8A-HLA-A2 in RMSD and TCR torsion angle coordinates

G) Free Energy Map in RMSD of the simulated unique metastable state structure of A6-TAX-HLA-A2 and TCR torsion angle coordinates

H) Schematic A6-Y8A-HLA-A2 structure for showing TCR torsion over the pMHC interface. TCR torsion was calculated as an angle between a line connecting two ends on MHC α1-helix (E54 and R81) and a line connecting centers of mass of TCR α and β variable domains.

Figure 5. Comparison of canonical A6-TAX-HLA-A2 signaling complex orientation and non-canonical unique metastable state interface.

A) Comparison of peptide conformation in X-ray structure of stimulatory A6-TAX-HLA-A2 (left) and unique metastable state of A6-TAX-HLA-A2 (right). The unique metastable TCR orientation is drastically different from canonical TCR orientation, resulting in a very different peptide conformation.

B) Distinct CDR positions in X-ray of stimulatory A6-TAX-HLA-A2 (left) and unique metastable state of A6-TAX-HLA-A2 (right) complexes. The metastable state is facilitated by changes in peptide presentation and MHC helix conformation resulting in a significant alteration of the pMHC interface allowing a novel mode of TCR recognition.

C) Close-up on MHC α1-helix kink stabilizing changes in TAX peptide backbone conformation in metastable state A6-TAX-HLA-A2. The peptide conformational change is facilitated by novel contacts between MHC helix residues His7- and His74 and oxygen of V7 residue of the peptide backbone.

TCR surface is shown as transparent; peptide backbone is grey, backbone nitrogen is dark blue, oxygen is red, peptide residues within 5 Å of TCR are cyan, peptide atoms within 3 Å of TCR are magenta, CDRs are shown as α-CDR-1 is green, α-CDR-2 is purple, α-CDR-3 is dark red, β-CDR-1 is yellow, β-CDR-2 is blue, β-CDR-3 is red. V7 and His70 and His 74 are yellow.

Figure 6. Interface comparison between signaling allogenic 42F3-QL9-H2-L^d and Non-signaling high-affinity 42F3-p3A1-H2-L^d complexes

A) X-ray of Signaling allogenic 42F3-QL9-H2-L^d vs non-signaling high-affinity 42F3-p3A1-H2-L^d
High-affinity synthetic peptide 42F3-p3A1-H2-L^d is a non-singling system with a unique non-canonical orientation

B) TCR orientation comparison X-ray of Stimulatory 42F3-QL9-H2-L^d vs unique Reverse state 42F3p3A1-H2-L^d
This unique presentation results in a significantly different TCR recognition mode.

TCR surface is shown as transparent, peptide backbone nitrogen is dark blue, oxygen is red, QL9 peptide is cyan, synthetic high-affinity p3A1 is orange, CDRs are shown as α-CDR-1 is green, α-CDR-2 is purple, α-CDR-3 is dark red, β-CDR-1 is yellow, β-CDR-2 is blue, β-CDR-3 is red.

Figure 7. The unique metastable state found in the syngeneic A6-TAX-HLA-A2 signaling complex is absent in allogenic 42F3-QL9-H2-L^d and 42F3-p3A1-H2-L^d complexes.

Theoretical 42F3-p3a1-H2-L^d orientation that is analogous to unique metastable state found in A6-TAX-HLA-A2.

Figure 8. **Free Energy Maps of stimulating 42F3-QL9-H2-L^d and non-stimulating 42F3-p3A1-H2-L^d complexes in RMSD and TCR torsion angle coordinates.**

A) Free Energy Map in RMSD derived from X-ray structure of 42F3-QL9 -H2-L^d and TCR torsion angle coordinates

B) Free Energy Map in RMSD derived from the theoretical unique metastable state structure of 42F3-QL9 -H2-L^d and TCR torsion angle coordinates

C) Free Energy Map in RMSD derived from X-ray structure of 42F3-p3a1-H2-L^d and TCR torsion angle coordinates

D) Free Energy Map in RMSD derived from simulated 42F3-p3a1-H2-L^d complex in the theoretical unique metastable state and TCR torsion angle coordinates

E) Schematic calculation of TCR torsion over the pMHC interface. TCR torsion was calculated as an angle between a line connecting two ends on MHC α1-helix (E54 and R81) and a line connecting centers of mass of TCR α and β variable domains.

2

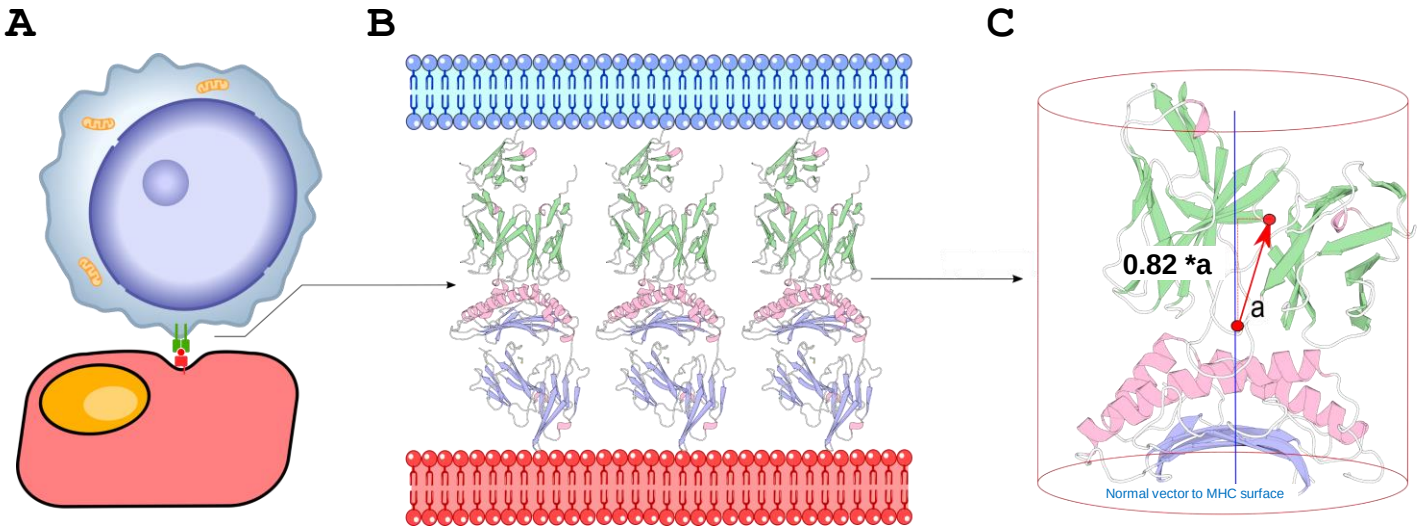

Figure 1

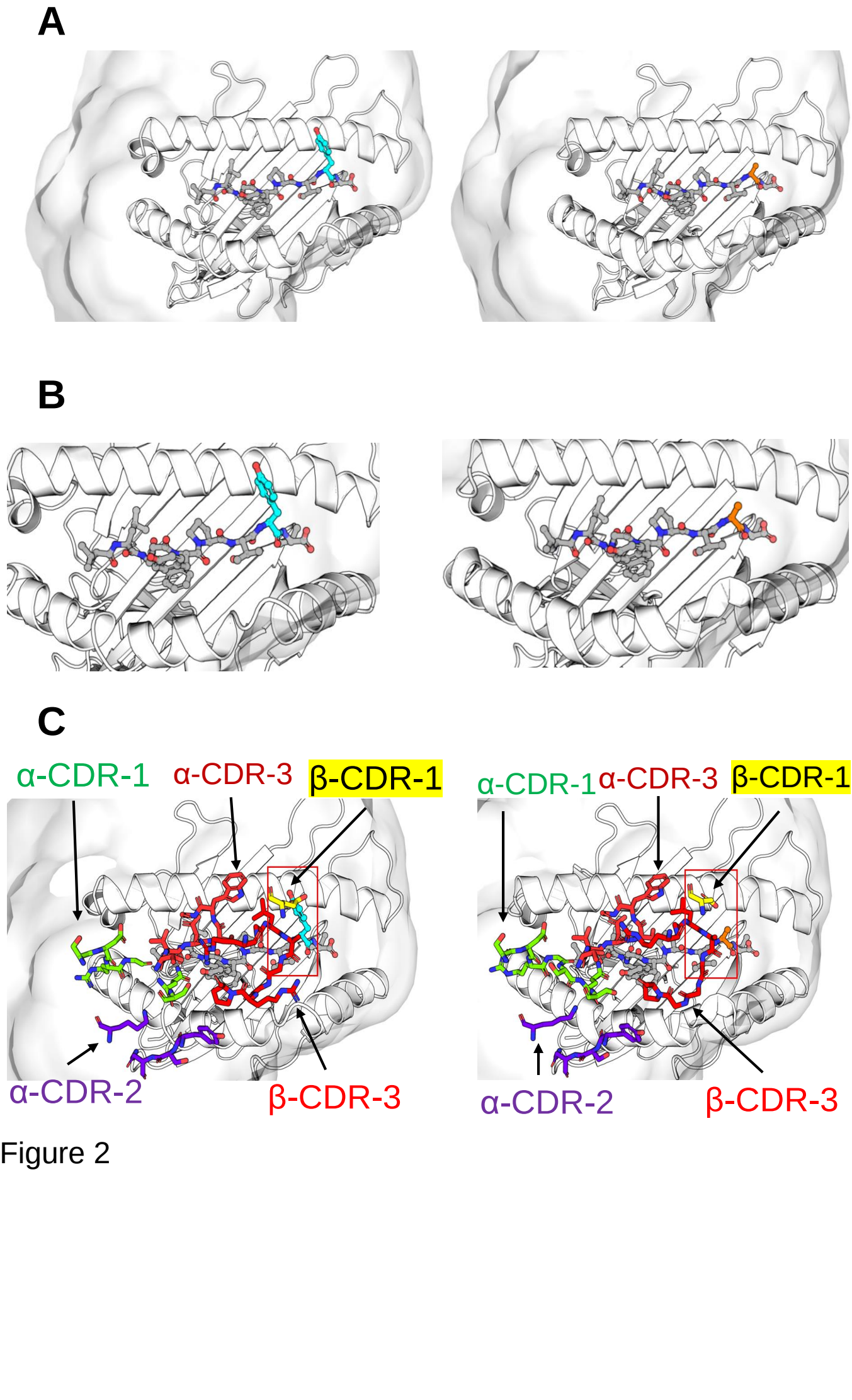

Figure 2

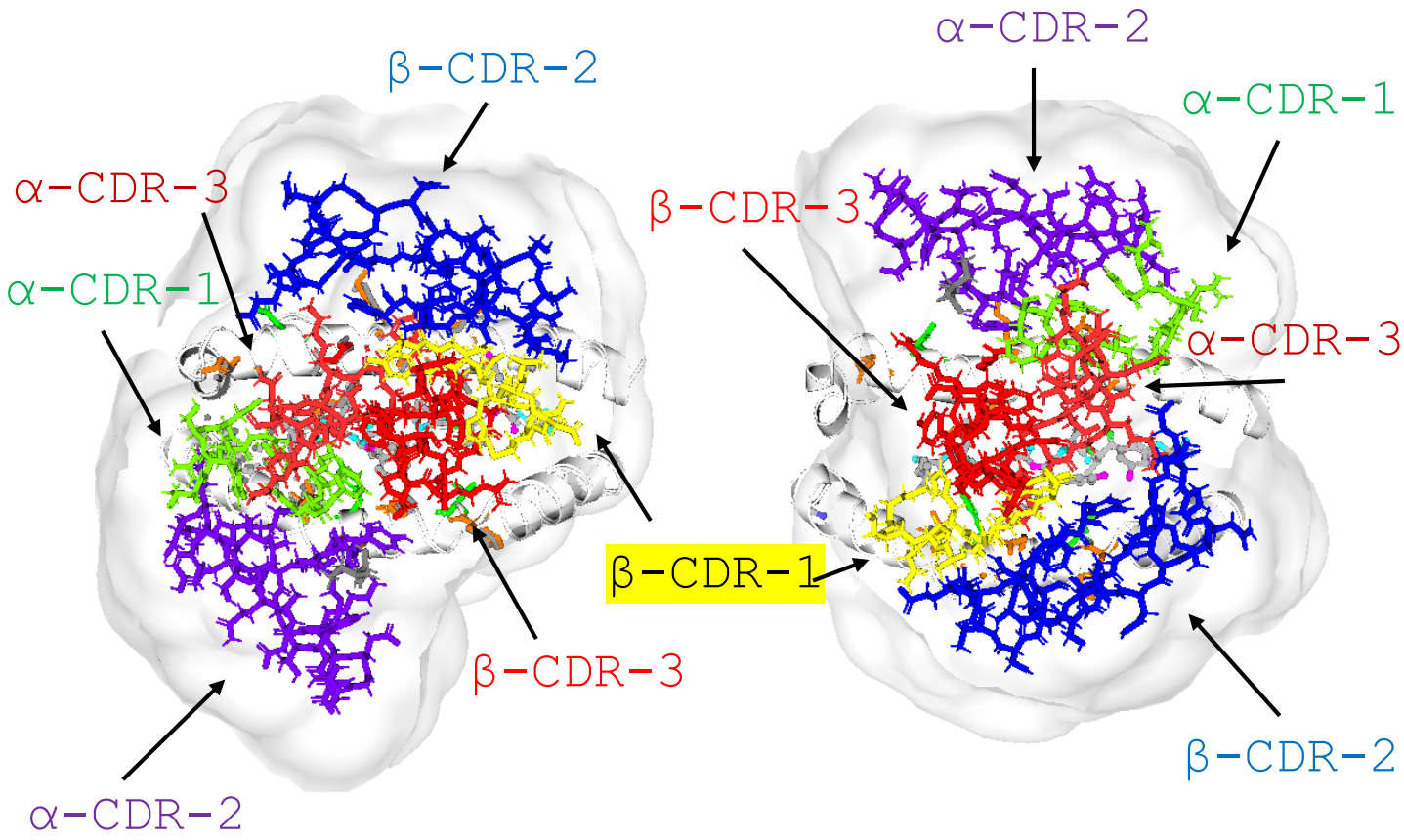

Figure 3

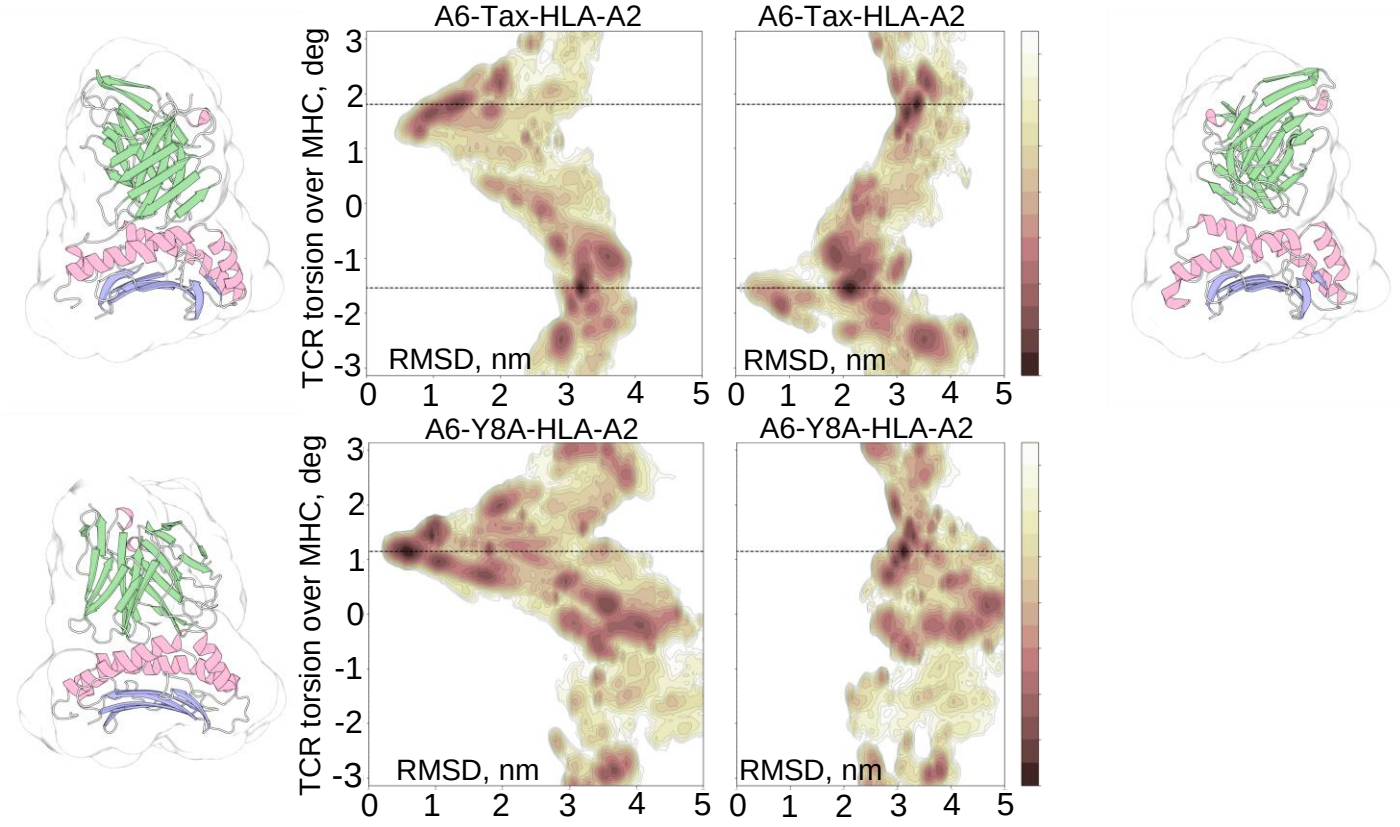

Figure 4

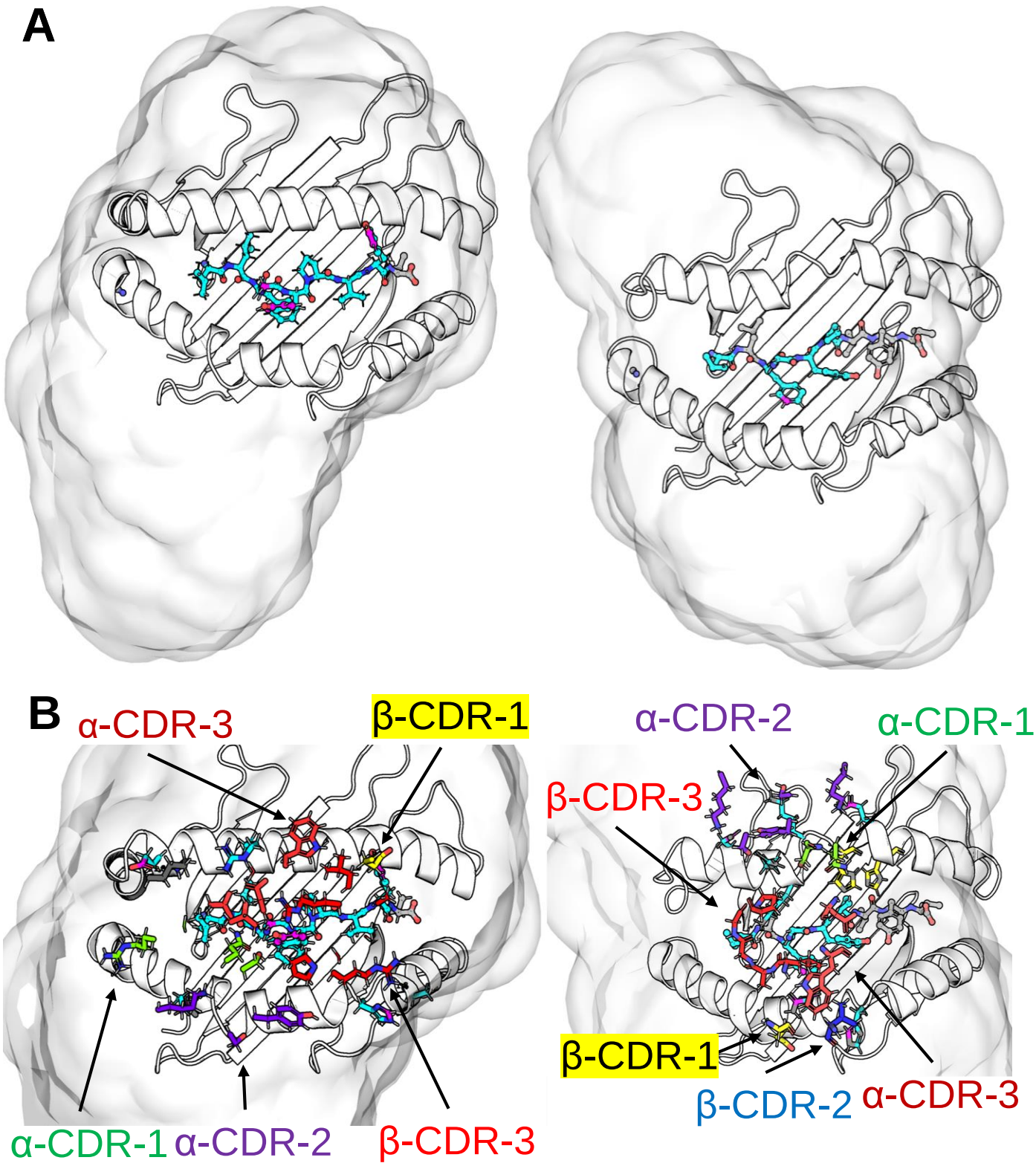

Figure 5

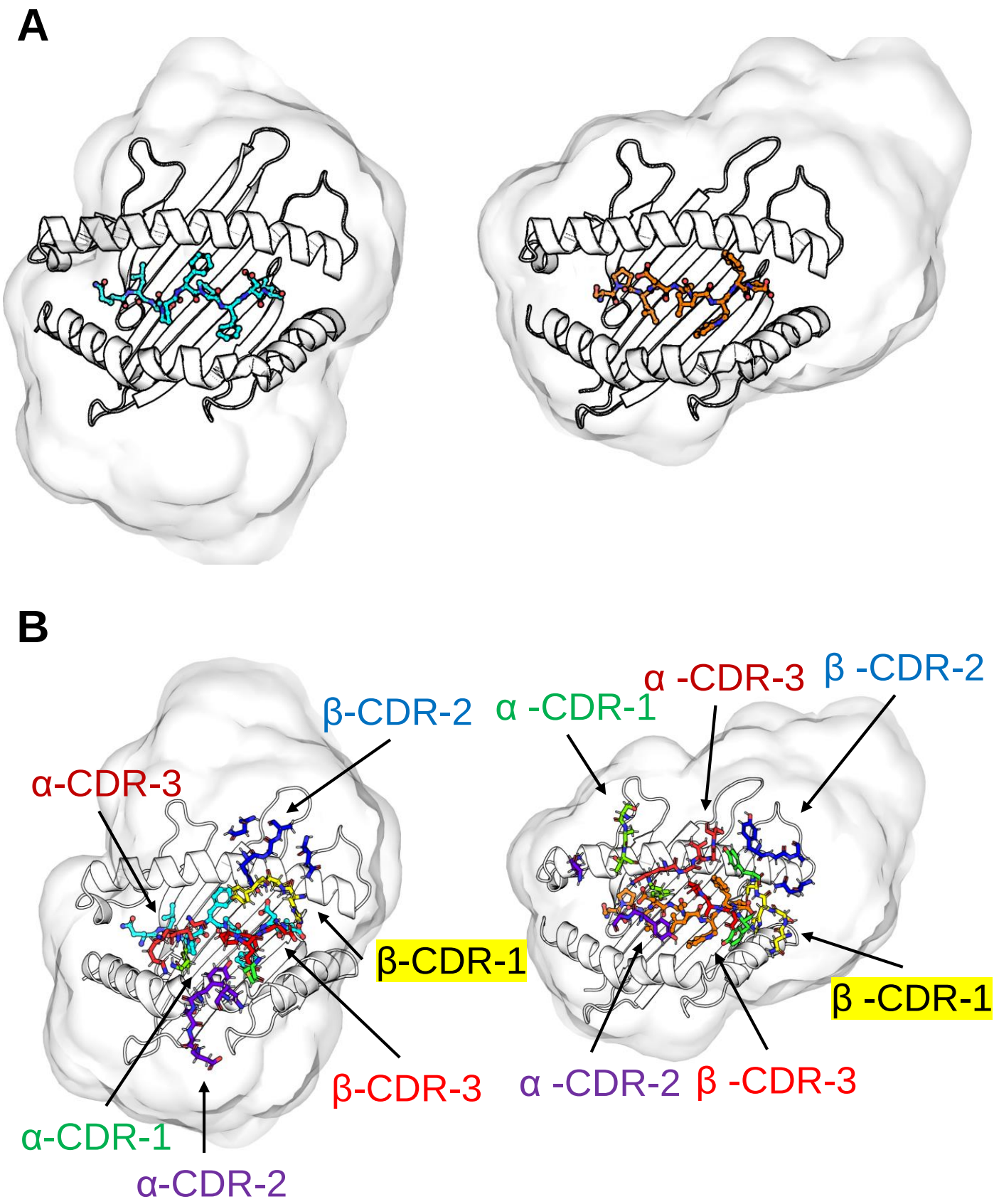

Figure 6

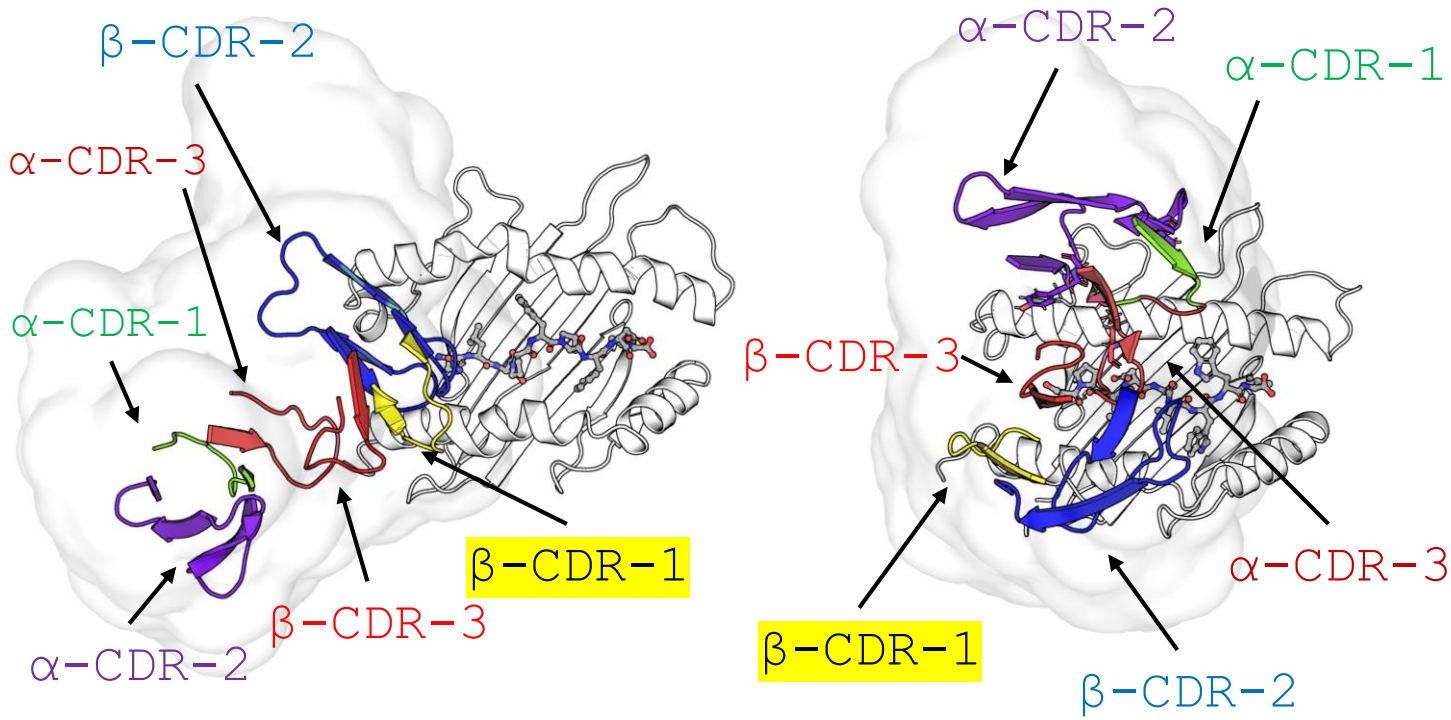

Figure 7

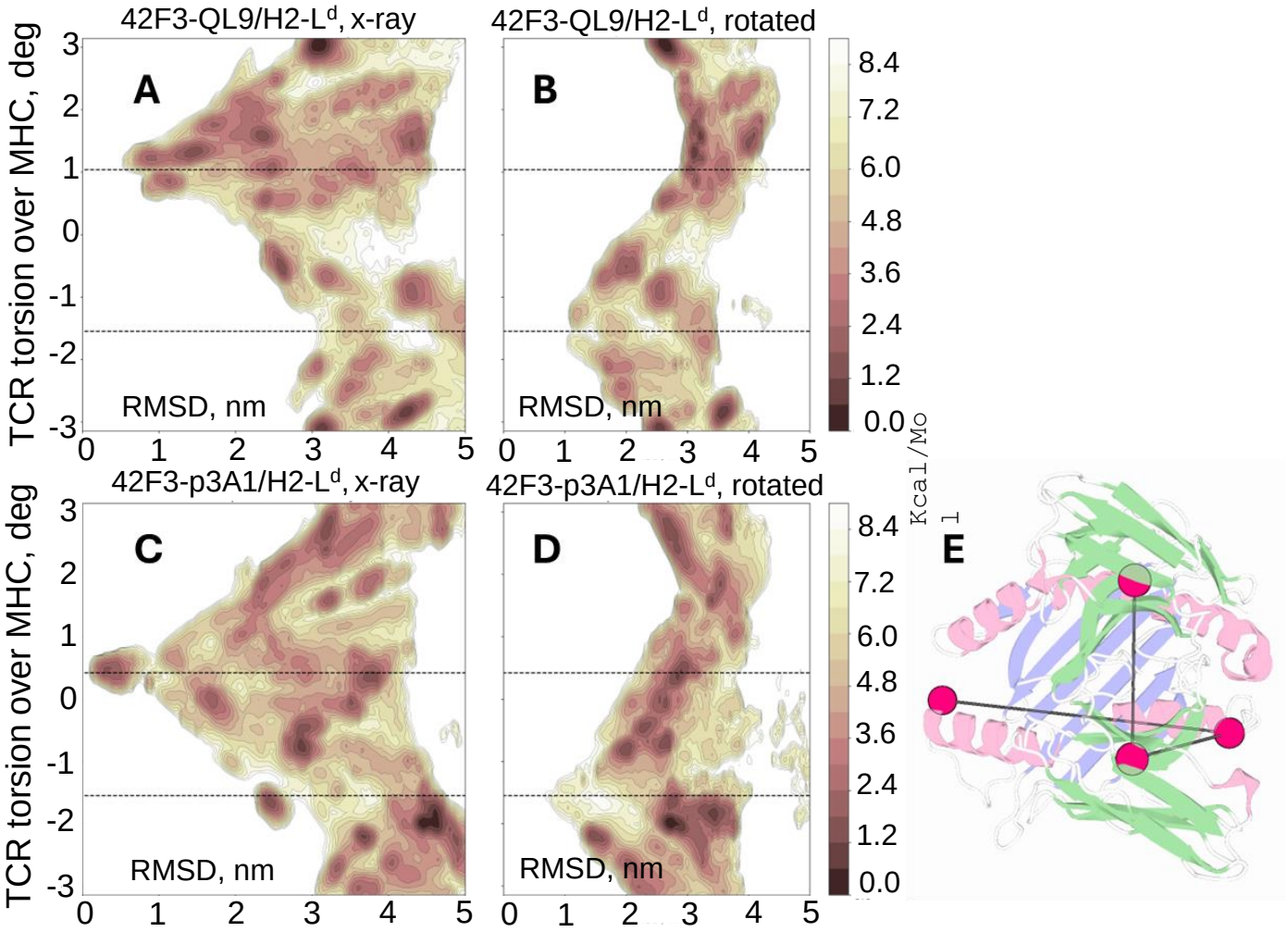

Figure 8

The authors declare no competing interests. All authors indicated that they don't have financial or other interests related to studies described in the manuscript.